J Solid State Electrochem (2010) 14:1967–1973
DOI 10.1007/s10008-009-1000-5

ORIGINAL PAPER

Application of classical and new, direct analytical methods for the elucidation of ion movements during the redox transformation of polypyrrole

Csaba Janáky · Gábor Cseh · Péter S. Tóth · Csaba Visy

Received: 30 November 2009 / Revised: 21 December 2009 / Accepted: 27 December 2009 / Published online: 23 January 2010

Abstract Redox transformation and related processes in conjugated polymers have been studied by both classical (electrochemical quartz crystal nanogravimetry, in situ optical electrochemistry and a. c. impedance technique) and modern, direct analytical methods. As a model, polypyrrole thin layers have been deposited on a double-band indium tin oxide-supporting electrode—for the first time in the literature. The structure of the printed circuit made possible to monitor simultaneously the electrochemical, the optical, and the conductance changes during the processes, occurring in the self-same film. The film has been deposited under similar conditions on a quartz crystal-supported platinum electrode, as well, to follow the mass changes. The oxidation state of the layers has been gradually modified by multiple potential steps, and the abovementioned measurements have been completed by elementary analysis performed by energy dispersive X-ray (EDX) spectroscopy. From the correlation of the results, obtained by independent methods, the mixed anionic and cationic charge compensation has been evidenced. While during the first part of the oxidation (−0.6 V to 0.0 V) cations are removed from the layer, in the second part (0.0 V-0.8 V) the anion incorporation is dominant. The results prove that EDX measurements can deliver direct semi-quantitative information on ion exchange processes accompanying the doping-undoping of conducting polymers.

Keywords Polypyrrole · Ionic movements · Spectroelectrochemistry · Conductance · EQCM · EDX

C. Janáky · G. Cseh · P. S. Tóth · C. Visy (✉)
Department of Physical Chemistry and Materials Science,
University of Szeged,
Aradi V. Sq. 1,
Szeged H-6720, Hungary
e-mail: visy@chem.u-szeged.hu

Introduction

The redox transformation of conjugated polymers is one of the most intensively studied phenomenon since the discovery of these materials in 1977 [1, 2]. As the process is coupled with conductance, spectral, mass, and volume changes, it is interesting—beyond the scientific importance—also from the point of applications. These changes can be exploited, among others, in smart windows, artificial muscles, sensors, and in micro valves and pumps [3–5]. Several studies have been published on the redox processes, where different analytical tools were combined with the electrochemical measurements in order to acquire independent information on the doping-undoping processes. Electrochemical quartz crystal microbalance (EQCM) is a powerful combined technique, which is able to deliver more complete information about the process, by measuring the mass changes related to ionic and non-ionic movements [6–10]. Electrochemistry have been successfully coupled with ultraviolet-visible spectroscopy (UV-vis) [11–13], electron spin resonance (ESR) [14, 15], Fourier transform infrared spectroscopy [16], Raman spectroscopy [17], probe beam deflection [18, 19], and atomic force microscope [20]. During recent years, in some cases two in situ methods have been applied simultaneously. This way ESR + AC impedance [21], ESR + UV-vis [22], AC electrogravimetry [23] and UV-Vis + AC impedance [24] combinations have been realized.

The nature of ionic and non-ionic movements during the redox transformation of conducting polymers is affected by various factors. Although, in principle both anionic and cationic movements can compensate the charges generated during the redox cycling, we have to take into account different factors, such as the size of the ions, their charge (monovalent or divalent) and their mobility (diffusion

coefficients) both in the solution and the polymer phase. In the first studies, the general assumption was that the counter ions (anions)—incorporated into the film during the polymerization—leave from and penetrate into the layer during the reduction and oxidation, respectively [25]. Later it has been proved that the phenomenon is more complex and it can be affected also by the present cations and the ion pairs as well [26–28]. Different studies proved that the contribution of anions and cations to the total charge compensation depends on both their size, the doping level and on the polymer itself [29–31]. Although there are contradictions in the literature, it is generally accepted that small-sized cations (pl. Li^+, Na^+, K^+) can be much more involved, compared to the bulky cations such as Bu_4N^+. However, this statement is not unambiguous, as the size of the ions and the whole process strongly depends on the solvation of the ions and the polymer [32]. It has been also demonstrated that ionic movements are influenced by the polymerization conditions of the film, due to structural differences caused by, e.g., the deposition potential [33]. It is important to point out that although several studies have been performed on the ionic movements in conducting polymers, there are only few approaches in which the moving species were directly identified [34–37].

In this work, our goal was to combine the results of the classical methods with complementary data available through novel analytical tools in order to get further, direct evidences on the ionic movement during the doping-undoping process of conducting polymers. Here, we report on the characterization of the redox transformation of polypyrrole in acetonitrile/Bu_4NBF_4 as a model system. The work is novel in two aspects: (1) we compare the results obtained by classical methods such as EQCM, in situ UV-vis spectro-electrochemistry, AC impedance with those measured by a modern elementary analysis technique, the energy dispersive X-ray (EDX) microanalysis. This method has been used earlier just for the qualitative characterization of the composition of the film [38]; (2) we applied two in situ electrochemical techniques to follow simultaneously the spectral and conductance changes in polypyrrole for the first time.

Experimental

Pyrroles (Py), tetrabutylammonium-tetrafluoroborate (Bu4NBF4), acetonitrile (AN) were purchased from Aldrich. The monomer was freshly distilled; the solvent was dried over 3 Å molecular sieves, and kept under inert atmosphere. The water content of the solutions was controlled by coulometric Karl Fischer titration, and was kept below 30 ppm.

Polypyrrole (PPy) was prepared galvanostatically at a current density of 3 mA cm^{-2}. The polymerization solution contained 0.1 M of the monomer pyrrole and 0.1 M Bu_4NBF_4 in AN. Different polymerization charge was controlled, and density was restricted to 60 mC cm^{-2} to avoid viscoelastic effects during EQCM measurements [39]. For the elementary analysis, EDX measurements have been performed. For this method, thicker layer have been synthesized, with a deposition charge density of 300 mC cm^{-2}.

All electrochemical measurements were performed on a PGSTAT 10 (Autolab) instrument, with a classical three-electrode electrochemical cell. The reference electrode was an Ag/AgCl electrode, having a potential 0.200 V vs. standard hydrogen electrode. Cyclic and linear voltammetric curves have been registered at different sweep rates between 10 and 100 mV s^{-1}, in a solution containing 0.1 M Bu_4NBF_4. During the multiple potential step experiments, the layers were conditioned at −1.0 V for 60 s, then the potential was stepped to −0.6/−0.4/−0.2/0.0/0.2/0.4/0.6/0.8 V and was kept there for 60 s in all cases.

During the simultaneous in situ spectral and impedance measurements, a special indium tin oxide (ITO)-coated glass electrode (IAME, Abtech) working electrode was applied. It consisted of 15 μm wide and 3 mm long needles, forming gaps of 15 μm width between neighboring electrode parts. When the polymer layer is forming on the ITO needle-shaped electrode, it covers the two identically polarized ITO needles to a height regulated by the solution level. Later, during the deposition, the film can grow over the 15 μm gap, forming electrical contact between the parts, so that conductance can be measured. The ITO-covered glass support makes possible optical transmission measurements. These in situ UV-vis-near infrared spectroscopic measurements were carried out by using an Agilent 8453 UV-visible diode array spectrophotometer in the range of 190–1,100 nm. The data obtained from AC impedance measurements at 130 Hz were analyzed by a lock-in amplifier (SR 830). The detailed description of the experimental setup was shown in our recent publication [24].

The EQCM measurements were performed using a quartz crystal resonator and analyser EQCM type 5510 (Poland). The crystals (f_0=10 MHz) were Pt coated and had a surface area of A=0.196 cm^2. The EQCM system was calibrated by electrochemical silver deposition using the standard procedure, and the value of −0.86 ng Hz^{-1} calibration constant was obtained for the crystal f_0=10 MHz.

Hitachi S-4700 scanning electron microscopy coupled with EDX spectroscopy (Röntec QX2) was used to obtain direct data for the elemental composition of the layers. EDX measurements were performed with a polymeric films deposited onto Pt electrodes. After the polymerization of the films, they were transformed in a solution containing 0.1 M Bu_4NBF_4, and (after a conditioning step at −1 V for 60 s) were kept at the selected potential for 60 s. Then, they

were immediately removed from solution, washed with AN, dried, and the proper analysis have been performed. All data presented in the figures have been obtained by averaging the results measured at three different areas of the films.

Results and discussions

In the first part of the studies, polypyrrole films were polymerized onto the double-band ITO glass, for making possible subsequent spectro-electrochemical studies during their redox transformations. We deposited very thin, homogeneous layers in order to follow the simultaneous spectral and conductance changes of the same film. Figure 1 demonstrates that the growth of the polymer is continuous even on the special printed circuit electrode. This process is indicated by the gradual development of the UV-vis spectra in the whole wavelength range. Relatively larger absorbance values, reached above 600 nm, prove that the polymer is formed in its oxidized state during the electropolymerization. The insert shows the continuous, fairly linear increase of the absorbance at two selected wavelengths. These wavelengths are related to the two characteristic forms of the polymer: the reduced (neutral) form at 450 nm and the oxidized form (bipolaron or dication) at 900 nm. Later, during the redox transition of the film, the absorbances measured at these wavelength values will be used to characterize the doping level of the polymers.

In order to investigate the mass changes connected to the doping-undoping processes, we carried out EQCM measurements during repetitive cycles run between the reduced and oxidized states. In Fig. 2, a representative voltammogram is shown, where the shape of the curve reflects to the good electroactivity of the freshly synthesized thin polypyrrole film. The cycling was started from the negative end of the potential window. The simultaneously recorded mass change curves reflect the complexity of the redox transformation. It is clearly visible that in the first section of the oxidation, a negative mass change can be detected, while from around E=0.0 V potential the mass starts to increase, which may indicate that from this point the oxidation is coupled by the incorporation of anions. In the second part of the cycle, i. e. during the reduction, first we can observe a mass decrease, related to the removal of anions from the layers, while by approaching the end of the scan, this decrease stops.

In order to get more information about the two different kinds of mass change, we repeated the voltammetric measurements at slower sweep rates by starting the scan from the oxidized state, after conditioning the film at the starting potential (E=0.7 V). The curves registered during a linear voltammetric measurement in Fig. 3 reflect a similar phenomenon as earlier, but the dual pattern of the mass change is more expressed, since there is a significant mass increase during the second part of the reduction.

To interpret these results we have to assume that, additionally to the anionic movements, cationic movements also take place, especially in the first part of the oxidation and the second part of the reduction (in the −0.6 to 0.0 V potential range). This is particularly interesting if we take into account that the Bu_4N^+ cation, due to its relatively large size, is not incorporating generally into the film.

In order to acquire more direct and reliable analytical information on the ionic movements, we decided to follow

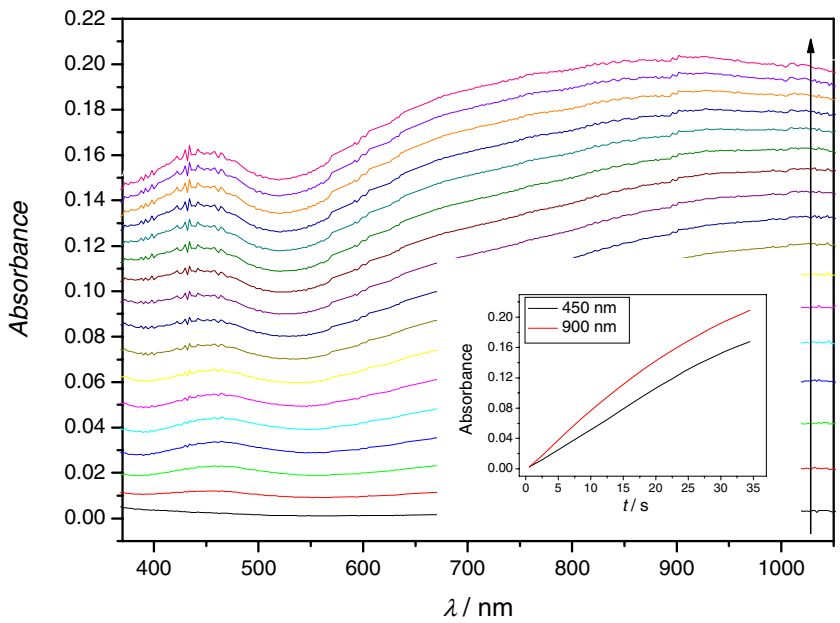

Fig. 1 UV-vis spectra recorded at each 2 s during the potentiostatic polymerization of pyrrole from a solution containing 0.1 M Py and 0.1 M Bu_4NBF_4 at a potential E=1.0 V. The *insert* shows the absorbance increase at two selected wavelengths

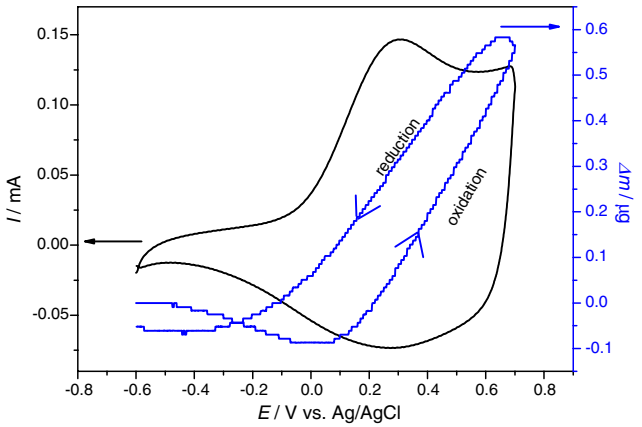

Fig. 2 Cyclic voltammogram of PPy recorded at 100 mV s^{-1} sweep rate in 0.1 M Bu_4NBF_4 in AN together with the mass change recorded by EQCM

these processes by EDX experiments. Since these measurements are ex situ, and we wanted to compare the results with those obtained by UV-vis spectroscopy and EQCM, we carried out combined potential step measurements. This way, we divided the oxidation process into eight parts by applying potential steps of 0.2 V each.

First, we followed the absorbance changes at the two selected wavelength, caused by the series of potential increase. Since we wanted to study the oxidation of the layer, we applied a 60 s pre-conditioning at −1.0 V, reducing the film completely. As it is expected, the two characteristic absorbances change oppositely during the oxidation process depicted in Fig. 4. While the optical density of the species registered at 900 nm increased step by step, the absorbance related to the reduced form of the polymer decreased by increasing the potential. It is also important to mention that significant spectral changes take place only above 0.0 V potential.

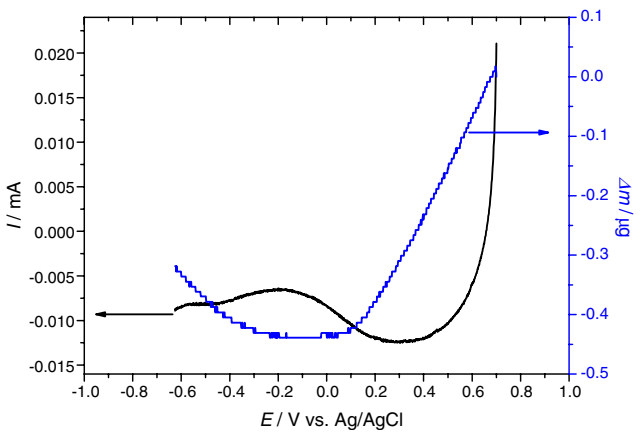

Fig. 3 Linear voltammogram of polypyrrole at 10 mV s^{-1}, started from 0.7 V in 0.1 M Bu_4NBF_4 in AN together with the mass change recorded by EQCM

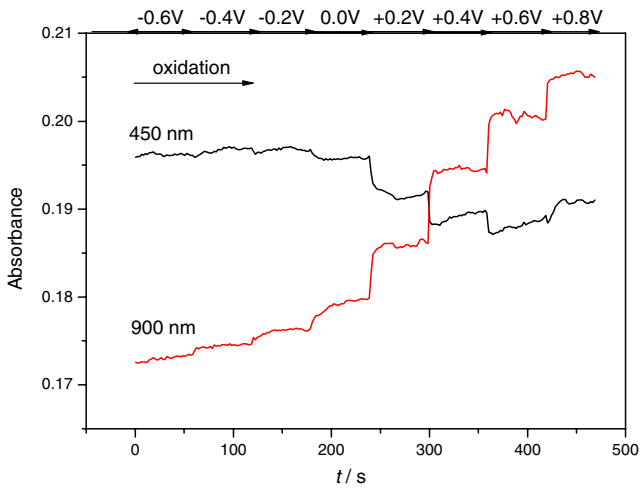

Fig. 4 Absorbance changes of polypyrrole during the potential steps between −0.6 V and +0.8 V at the two selected wavelengths

As a next step, similar potential step measurements have been performed by using the EQCM technique and we followed the global mass changes during the oxidation. The results are in perfect agreement with those obtained by voltammetry. As it can be seen in Fig. 5, where the cumulative mass change is shown as a function of the applied potential, first the mass is decreasing in the potential range between −0.6 and 0.0 V, while it starts to increase above this potential. It is important to emphasize that in the first potential range, we can measure only small currents (the overall charge is very small), while the detected mass change (Δm_1=50 ng) is relatively large. It is even more striking if we compare it to the not too much larger mass increase during the second section of the oxidation process (Δm_2=200 ng), which is related to significantly larger oxidation charge. This observation, which confirms the involvement of cations into the doping process, can be

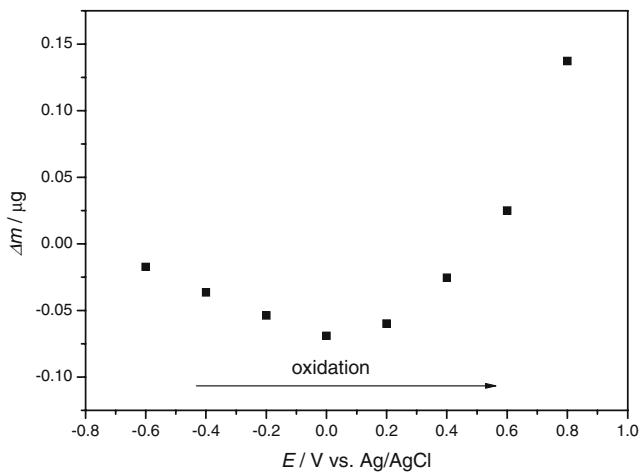

Fig. 5 The overall mass change during the potential step measurements between −0.6 V and 0.8 V for PPy in 0.1 M Bu_4NBF_4 in AN

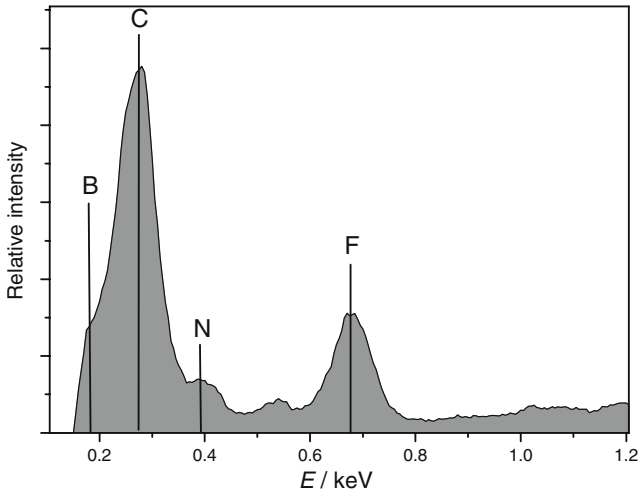

Fig. 6 EDX spectrum of a PPy layer synthesized galvanostatically, at a current density of j=3 mA cm^{-2} and at a charge density of 300 mC cm^{-2}

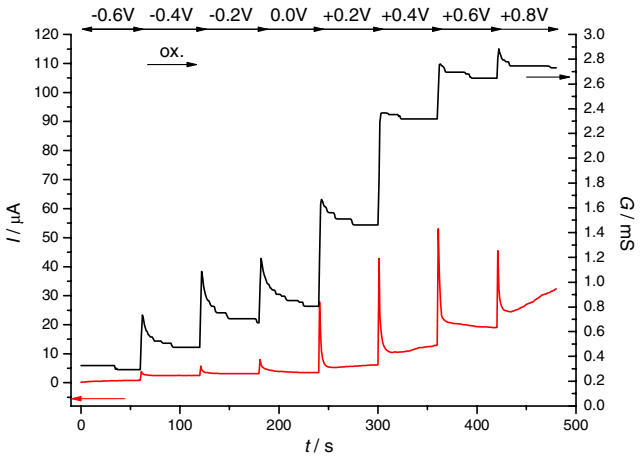

Fig. 8 Current transients and conductivity changes of PPy during the potential steps between −0.6 V and 0.8 V for PPy in 0.1 M Bu_4NBF_4 in AN

related first of all to the difference in the molar masses of BF_4^- and Bu_4N^+.

In order to get direct information on the chemical composition of the polymeric films—with different doping level—we carried out EDX experiments. Before the analytical measurements, the layers were conditioned at −1.0 V for 60 s, after they were kept at the selected potential for 60 s, and after their removal from the solution they were washed and dried. A selected part of a typical spectrum is visible in Fig. 6. It clearly proves that the film contains BF_4^- anions, unfortunately the peak related to boron is very close to (and emerged into) the large carbon peak. For this reason, we cannot use it for quantitative purposes. In contrast, Fluor can be detected as a separate peak and can be used to indicate the incorporation and amount of tetrafluoroborate anions during the oxidation. As for the amount of Bu_4N^+ cations, we do not have direct information, since polypyrrole also consists of C, N, and H. However, the eventual modification of the C/N ratio may reflect the changing amount of the cations in the polymer layer. In order to get comparable data, we have to ensure that the polymer thickness is at least similar in all cases; otherwise, we could not compare the relative F contents. As we synthesized the layers with the same charge density, we expected to have similar thicknesses. This was proved by the EDX measurements themselves, as the signal of the Pt-supporting electrode was similar in all cases (3.6±1.2 at.). This also means that the total amount of the elements originating from the polymeric layer was dominant and similar in all measurements (96.4±1.2 at.). Thus, we can directly compare the relative F amounts obtained in the different samples.

In order to quantify the ionic movements based directly on the EDX data, we present the relative amount of F in

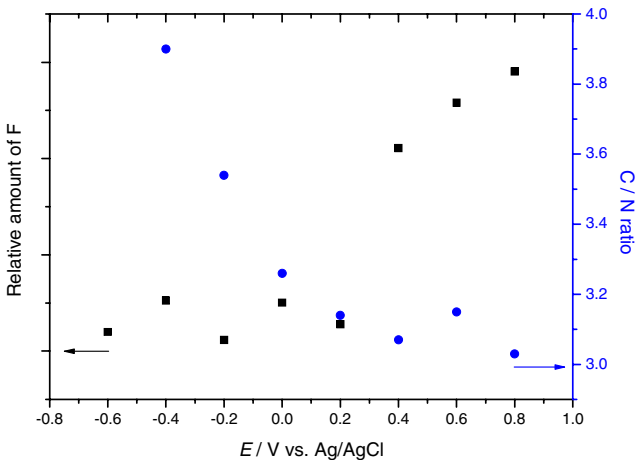

Fig. 7 Comparison of the relative amount of F and C/N ratio for the PPy layers conditioned at eight different potentials

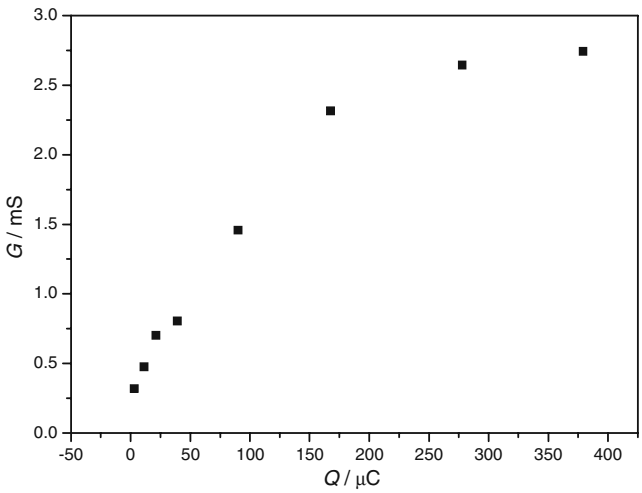

Fig. 9 Conductivity increase as a function of the cumulative charge transferred during the potential step measurements presented in Fig. 8

parallel with the C/N ratio. The results obtained for the polymers conditioned to stabilize their different oxidation states at eight different potentials are shown in Fig. 7. The first interesting point that one can observe is that both signals change drastically around 0.2 V. This coincidence confirms the correctness of our previous assumptions. As it is visible, the relative amount of F is almost constant in the first part of the oxidation. This observation is convincing from the point of view of the reproducibility since we analyzed different films in each case. The amount of the detected Fluor, however, starts to increase dramatically from 0.2 V. This is in agreement with the EQCM results confirming that the anion incorporation takes place in the second part of the oxidation. As for the C/N ratio, oppositely, it is constant during the second part of the oxidation, while it exhibits a significant decrease in the first section. Since the C/N ration is constant in the polymer itself, this observation cannot be explained otherwise, but excludingly by the removal of the "C-rich" Bu_4N^+ cations. It is important to mention that in case of the C/N ratio—as the analysis of the N-peak is rather difficult—not the exact value, but its tendency is important. Thus, the assumption, made on the basis of the results obtained by the "classical" analytical methods has been confirmed. Direct analytical data approved that the charge compensation is modifying during the redox process: in the first part of the oxidation, cationic movements are dominant, and anionic movements take place only at more positive potentials.

The use of the double-band ITO electrode made possible that we could complete our results also with in situ AC impedance data measured during the potential steps, parallel to the UV-vis measurements. With this method, we get information on the name-giving property of these materials as we measure the conductance of the sample in different oxidation states. In Fig. 8, we compare the current transients and the conductivity increments caused by them for each 200 mV potentials step. It is clearly visible that in the first part of the oxidation, the small currents (and charges) are coupled with relatively large conductance increases. At the same time, the large currents in the second part results in relatively smaller increments, especially during the two last steps.

This qualitative picture can be quantified, if we present the conductivity versus the cumulative charge, passed through during the potential steps. As it can be seen in Fig. 9, the conductivity is increasing more rapidly in the first part of the oxidation, while after ~80 μC (during the second part of the oxidation) the growth is moderate and the conductance tends to reach a saturation value. If we take into consideration the relation between the results obtained for the ionic movements and the conductivity change, we may conclude that the rapid change in the conductivity is related to the cation removal from the layer, while during the anion incorporation, the conductance increases much slower.

Conclusions

The results prove that data obtained for the redox transformation by classical methods could be completed by direct elementary analysis results. EDX measurements clearly evidence that beside the incorporation of tetrafluoroborate anions also the removal of cations occurs during the oxidation of the film. The process is reversible in the sense that opposite charge compensation processes can be detected during the discharge of the polymer film. Correlation between the results obtained by independent methods confirms that the relatively small oxidation charge is connected to the removal of cations, which can be directly connected to the decrease in the C/N ratio in the film. Thus, bulky tetrabutylammonium ions are incorporated into the film, although their presence in the polymer layer and their involvement into the charge compensation process is generally let out of consideration. The release of cations can result in a faster increase in the conductance of the film, while in the second section of the redox-switching process, the incorporation of anions is accompanied by a much slower conductivity change. If we compare the charge transferred in connection with the different ionic movements, we may conclude that in the second part of the transformation relatively less charge is consumed for the increase of the conductance. One-half of the conductance increase is dominantly related to the cation removal, but it is connected to only one quarter of the transferred charge.

It is strongly believed that further studies based on simultaneous recording of the optical spectra and the conductance—which technique is applied here for the first time to monitor the redox-switching process of polypyrrole—may open opportunity to correlate the development and sustenance of the conducting state with the differently absorbing charge carriers and perhaps to the different ions participating in the charge compensation.

Finally, investigation of this model system clearly proves that EDX is a powerful technique to characterize conducting polymer films and to get direct semi-quantitative data on the amount of dopants/co-ions in the polymers at different oxidation levels. This way, it opens the opportunity not only to follow the ionic movements, but EDX can simultaneously quantify both cationic and anionic species involved in the charge compensation.

Acknowledgment Financial support from the Hungarian National Research Fund (OTKA no. K72989) is gratefully acknowledged.

References

1. Shirakawa H, Louis EJ, MacDiarmid AG et al (1977) J Chem Soc, Chem Commun 16:578

2. Bredas JL, Themans B, Fripiat JG, Andre JM, Chance RR (1984) Phys Rev B 29:6761
3. Inzelt G (2008) Conducting polymers, a new era in electrochemistry. Monographs in electrochemistry. Springer-VBH, Leipzig
4. Andrews MK, Jansen ML, Spinks GM et al (2004) Sens Actuators A Phys 114:65
5. Ramanavicius A, Ramanaviciene A, Malinauskas A (2006) Electrochim Acta 51:6025
6. Hillman AR, Swann MJ, Bruckenstein S (1990) J Electroanal Chem 291:147
7. Inzelt G (1990) J Electroanal Chem 287:171
8. Bruckenstein S, Brezinska K, Hillman AR (2000) PCCP 2:1221
9. Plieth W, Bund A, Rammelt U et al (2006) Electrochim Acta 51:2366
10. Inzelt G, Kertesz V, Nyback AS (1999) J Solid State Electrochem 3:251
11. Visy C, Lukkari J, Pajunen T, Kankare J (1989) Synth Met 33:289
12. Carlberg C, Chen XW, Inganas O (1996) Solid State Ionics 85:73
13. Arjomandi J, Holze R (2007) J Solid State Electrochem 11:1093
14. Matenzio T, Vieil E (1991) Synth Met 44:349
15. Genies EM, Lapkowski M (1987) J Electroanal Chem 236:199
16. Zerbi G, Radaelli R, Veronelli M, Brenna E, Sannicolo F, Zotti G (1993) J Chem Phys 98:4531
17. de Tacconi NR, Son Y, Rajeshwar K (1993) J Phys Chem 97:1042
18. Vilas-Boas M, Henderson MJ, Freire C, Hillman AR, Vieil E (2000) Chem Eur J 6:1160
19. Matencio T, Depaoli MA, Peres RCD et al (1995) Synth Met 72:59
20. Skompska M, Szkurlat A, Kowal A et al (2003) Langmuir 19:2318
21. Waller AM, Compton RG (1989) J Chem Soc, Faraday Trans 85:977
22. Rapta P, Faber R, Dunsch L, Neudeck A, Nuyken O (2000) Spectrochim Acta A 56:357
23. Gabrielli C, Perrot H, Rubin A, Pham MC, Piro B (2007) Electrochem Commun 9:2196
24. Peintler-Krivan E, Toth PS, Visy C (2009) Electrochem Commun 11:1947
25. Diaz AF, Castillo JI, Logan JA, Lee WY (1981) J Electroanal Chem 129:115
26. Naoi K, Lien M, Smyrl WH (1991) J Electrochem Soc 138:440
27. Heinze J, Bilger R (1993) Ber Buns Ges-Phys Chem Chem Phys 97:502
28. Vorotyntsev MA, Vieil E, Heinze J (1998) J Electroanal Chem 450:121
29. Levi MD, Lopez C, Vieil E, Vorotyntsev MA (1997) Electrochim Acta 42:757
30. Weidlich C, Mangold KM, Juttner K (2005) Electrochim Acta 50:1547
31. Manogil PP, Fernández Romero AJ J Solid State Electrochem
32. Visy C, Janaky C, Krivan E (2005) J Solid State Electrochem 9:330
33. Vorotyntsev MA, Vieil E, Heinze J (1996) Electrochim Acta 41:1913
34. Horanyi G, Inzelt G (1988) Electrochim Acta 33:947
35. Qi ZG, Pickup PG (1993) Anal Chem 65:696
36. Bach CMG, Reynolds JR (1994) J Phys Chem 98:13636
37. Briseno AL, Baca A, Zhou Q, Lai R, Zhou F (2001) Anal Chim Acta 441:123
38. Fernandez-Romero AJ, Lopez Cascales JJ, Otero TF (2005) J Phys Chem B 109:907
39. Skompska M, Jackson A, Hillman AR (2000) PCCP 20:4748